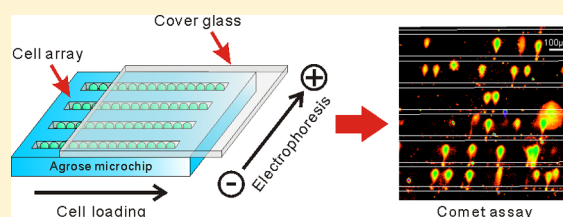


# Ultrahigh-Throughput Approach for Analyzing Single-Cell Genomic Damage with an Agarose-Based Microfluidic Comet Array

Yiwei Li, Xiaojun Feng, Wei Du, Ying Li, and Bi-Feng Liu\*

Britton Chance Center for Biomedical Photonics at Wuhan National Laboratory for Optoelectronics—Hubei Bioinformatics and Molecular Imaging Key Laboratory, Systems Biology Theme, Department of Biomedical Engineering, College of Life Science and Technology, Huazhong University of Science and Technology, Wuhan 430074, China

**ABSTRACT:** Genomic DNA damage was generally identified with a “comet assay” but limited by low throughput and poor reproducibility. Here we demonstrated an ultrahigh-throughput approach with a microfluidic chip to simultaneously interrogate DNA damage conditions of up to 10 000 individual cells (approximately 100-fold in throughput over the conventional method) with better reproducibility. For experiment, agarose was chosen as the chip fabrication material, which would further act as an electrophoretic sieving matrix for DNA fragments separation. Cancer cells (HeLa or HepG2) were lined up in parallel microchannels by capillary effect to form a dense array of single cells. After treatment with different doses of hydrogen peroxide, individual cells were then lysed for subsequent single-cell gel electrophoresis in the direction vertical to microchannel and fluorescence detection. Through morphological analysis and fluorescent measurement of comet-shaped DNA, the damage conditions of individual cells could be quantified. DNA repair capacity was further evaluated to validate the reliability of this method. It indicated that the agarose-based microfluidic comet array electrophoresis was simple, highly reproducible, and of high throughput, providing a new method for highly efficient single-cell genomic analysis.



With the emerging of systems biology, high-throughput analytical technologies have gained tremendous development.<sup>1,2</sup> It greatly facilitates current genomic, proteomic, and metabolomic researches,<sup>3–5</sup> particularly at single-cells level.<sup>6–8</sup> For example, single-cell genomic sequencing has developed rapidly in recent years, thanks to advancement of micro/nanofluidic chips and single-molecular detection.<sup>9–16</sup> Single-cell investigation features low sample requirement, low cost, and high efficiency. However, the challenge to high-throughput single-cell analysis still remains.

Genomic DNA damage is a universal phenomenon occurring when individual cells are exposed to varied damage sources such as reactive oxygen species, ultraviolet light, or viruses. DNA repair capability of individual cells ensures the accurate transmission of genetic information and the survival of species.<sup>17–22</sup> Knowledge about DNA damage provides us a better understanding of the molecular mechanism behind cancer, aging, and heritable diseases, which can further help us predict the risk of cancer and provide a new perspective to therapeutics or even find novel pathological targets.

Traditionally, genomic DNA damage is mainly investigated with a single-cell gel electrophoresis termed “comet assay”, introduced 2 decades ago.<sup>23–25</sup> The principle of comet assay is based on DNA strand breaks and the relaxation of the DNA supercoil. Genome DNA is separated by gel electrophoresis, and the comet-shaped DNA is visible using fluorescence microscopy. Through morphological analysis and fluorescence measurement of comet-shaped DNA, the DNA damage of individual cells could be quantified. The head of the comet contains the high-molecular-weight DNA, while the tail of the comet contains the

migrated DNA fragments and uncoiled DNA loops. Thus, the distribution of DNA in the tail represents the percentage of damaged DNA. Comet assay has been expanded to many application fields such as human biomonitoring, gene–environment interactions, drug screening, and genotoxicity testing. It has advantages of low cost and ease of access.<sup>26–31</sup> In addition, the results of comet assay reflect the integrated cellular response to different extracellular environments.

However, comet assay has limitations of low throughput and poor reproducibility. Many efforts have been made to improve this method. Recently, Wood et al. developed a microwell array, in which single cells were captured by gravity into the agarose wells to ensure that comets were spatially encoded.<sup>32</sup> It enabled simultaneous assays of multiple experimental conditions in parallel with automated analysis. Mercey et al. developed a three-dimensional (3D) micropatterning of agarose substrate for cell culture and in situ comet assays.<sup>33</sup> One or more cells were cultured on the patterned agarose where extracellular matrix proteins were grafted. The 3D patterned culture slides were also suitable for high-throughput comet assay. More recently, a HaloChip was employed by Qiao et al. for single-cell DNA damage/repair assay as a variant of comet assay.<sup>34</sup>

The microfluidic chip, referred to as a lab-on-a-chip, has recently been highly focused, due to advantages of low cost, high throughput, integration, and automation capability. It allows the measurements arranging from molecules and cells to small

Received: January 10, 2013

Accepted: March 11, 2013

Published: March 11, 2013

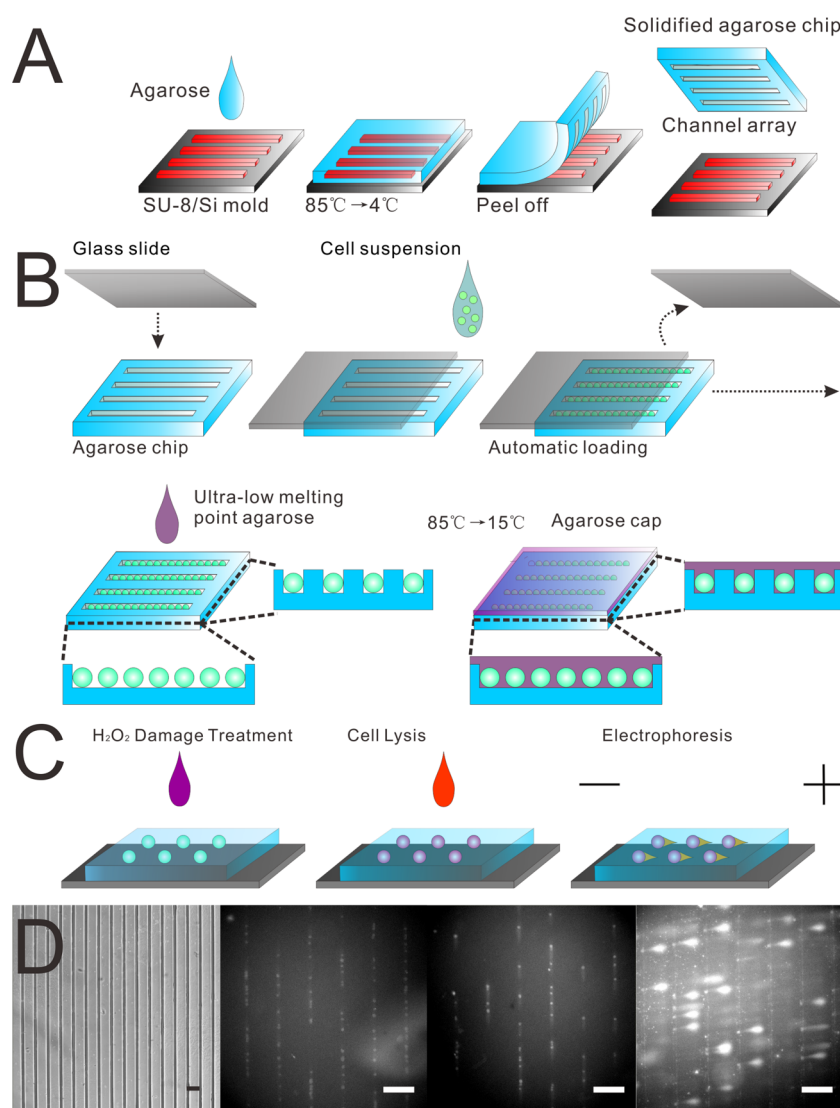


**Figure 1.** Passive formation of a single-cell array for comet assay. (A) Schematic of chip fabrication. (B) Cell loading. The agarose chip was covered with a glass slide cover (ensuring one end of the channel is open). A droplet of cell suspension was pipetted into the inlet. The cells flowed into the channel passively and lined in the channel one by one with capillary effect. Finally, the glass was removed and a droplet of 1% ultralow melting agarose was pipetted on the top of the chip to seal the channel array. (C) Schematic of the comet assay. The cell array sealed in the chip was treated with DNA damage agent and then submerged in the lysis solution. After that, electrophoresis was conducted under alkaline conditions. (D) Experimental results of the comet assay. Figures from the left to right represent the agarose chip under bright field, the fluorescence image after the cells were loaded into the channel array, chip comet electrophoresis inside the channels, and comet electrophoresis perpendicular to the channel, respectively.

organisms and has been recognized as the next-generation platform toward systems biology.<sup>35–44</sup> The microfluidic chip is an ideal platform for single-cells analysis.<sup>36,45–50</sup> The microchannel has compatible size with a regular cell. Precise microflow control enables versatile cell operations such as cell transportation, sorting, docking, localization, solubilization, and subsequent cell lysate analysis. The application of microfluidics for genetic analysis has also been extensively studied.<sup>51–58</sup> However, no report has been found to use a microfluidic chip for achieving a high-throughput comet assay.

In this paper, we demonstrate a novel microfluidic comet array electrophoresis method for ultrahigh-throughput genomic DNA analysis at single-cells level. The microfluidic chip was uniquely fabricated using agarose with an array of 100 parallel channels. The size of the microchannel was 20  $\mu\text{m}$  both in width and in height, which allowed only one cell to pass through at one time. After the cell suspension was pipetted into the inlet of the

microchannels, single cells were loaded into the channels array passively by capillary effect. Individual cells were closely packed in a linear configuration in the microchannels, and single-cell arrays were formed automatically in less than 5 min. The localized single cell was then lysed. The released genomic DNA was subject to agarose gel electrophoresis. We used this novel agarose-based microfluidic comet assay to measure the genome damage of HeLa and HepG2 cells in high throughput under different DNA damage conditions. Results indicated the heterogeneity in a cell line. We further employed this chip to study cell repair capability. Results showed that DNA repair could be finished within an hour. With this method, over 10 000 individual cells could be measured on a 25 mm  $\times$  25 mm agarose chip simultaneously with an available cell array density of 25 comets/ $\text{mm}^2$ , which is 100-fold higher than the throughput of the traditional method as reported. The agarose-based microfluidic comet array electrophoresis is simple, highly reproducible,

robust, and, more importantly, high-throughput, providing a new method for single-cell genomic analysis.

## MATERIALS AND METHODS

**Materials and Reagents.** Chemicals such as agarose,  $K_2HPO_4$ ,  $KH_2PO_4$ , KI,  $H_2O_2$ ,  $Na_2EDTA$ , NaOH, NaCl, and sodium lauryl sarcosinate were purchased from Sinopharm Chemical Reagent (Shanghai, China). DNA fluorescent dye (propidium iodide) was purchased from Beijing Biosynthesis Biotechnology Co., Ltd. (Beijing, China). Ultralow melting point agarose was obtained from Sigma-Aldrich (U.S.A.). Propidium iodide of concentration 2.5  $\mu\text{g}/\text{mL}$  was used to stain DNA. Alkaline solution (1.2 M NaCl, 100 mM  $Na_2EDTA$ , 1 g/L sodium lauryl sarcosinate, 0.26 M NaOH, pH > 13) was used for cell lysis. Solution containing 0.03 M NaOH, 2 mM  $Na_2EDTA$  (pH = 12.3) was prepared for rinsing and electrophoresis. Gradient hydrogen peroxide solutions were dissolved in phosphate buffer solution (pH = 7.4), used as DNA damage agents. Water used for all the solutions preparation was purified by the Direct-Q system (Millipore, Bedford, MA, U.S.A.) and filtered with 0.45  $\mu\text{m}$  sterilized syringe filters prior to use.

**Cell Culture.** HeLa, HepG2, and HeLa CD-3 cell lines were cultured in culture flasks (BD Falcon) containing 5 mL of DMEM medium with 10% (v/v) fetal bovine serum, 100 U/mL penicillin, and 100  $\mu\text{g}/\text{mL}$  streptomycin. All cell lines were incubated (5%  $CO_2$ , 90% humidified) at 37 °C in an incubator (Innova-Co 170; New Brunswick Scientific, U.K.) prior to use. Cells were subcultured at a ratio of 1:3 every 3 days to maintain cells in the exponential growth phase. Cells were detached from the flask with the treatment of 0.25% (w/v) trypsin–EDTA solution (Gibco) for 3 min for harvest. Cells were then suspended in the culture media at a concentration of  $1 \times 10^5$  cells/mL before use.

**Fabrication of Agarose-Based Microfluidic Chip.** The fabrication method of agarose chips was similar to the rapid poly(dimethylsiloxane) (PDMS) prototyping method as shown in Figure 1A. The SU-8 1070 (Gersteltec Sarl, Switzerland) mold was fabricated using soft lithography on a silicon wafer (n-type <100>). The agarose layer, made from 2% (w/v) normal melting point agarose, was fabricated by molding the SU-8 channel array. After being cured at the room temperature for 20 min, the agarose sheet was peeled from the mold. The patterned agarose sheet was then covered with a glass slide to form the final device. One of the arrayed channel ends was used as the cell inlet, while the other was closed as shown in Figure 1B.

**Cell Loading Procedure.** A novel loading system based on capillary effect was demonstrated to arrange distinct cells in specific, predefined patterns in the agarose-based chip. To prevent overlap of comets, cell density was adjusted to about  $1 \times 10^5$  cells/mL in phosphate-buffered solution. Cell suspension of 100  $\mu\text{L}$  was pipetted to the inlet of the channels, and the cells were loaded into the microchannels by capillary effect. The size of the channels was 20  $\mu\text{m}$  both in width and in height to allow only one cell passing through at a time. Cells were stopped at the end of the channels but not the solution due to the good water permeability of the agarose gel. More cells flowed into the microchannels, and the cells were collected in a linear configuration in the microchannels to form an array of cells. The whole process was passive without any external energy, avoiding external stress-induced cell response (Figure 1B).

**Genome Damage and Microfluidic Chip Comet Assay.** After cells were loaded, the chip was set aside for a few minutes. The coverglass slide was removed, and the chip was sealed with

0.5% (w/v) ultralow melting temperature agarose. After the agarose became solid, the chip was submerged into gradients of hydrogen peroxide solutions for 7 min. The chip was rinsed with rinse solution to remove the residual hydrogen peroxide. Then the chip was submerged into lysis solution overnight (18–20 h) in the dark at 4 °C. The chip was taken out of the container gently and submerged into rinse solution for 20 min three times to remove salt and detergent. For electrophoresis, the chip was submerged in an electrophoresis chamber that contained alkaline electrophoresis solution. The current was adjusted to 40 mA. Electrophoresis perpendicular to the channels (the fourth picture in Figure 1D) was chosen for less overlaps of comets and higher throughput compared with electrophoresis inside the channels (the third picture in Figure 1D). After electrophoresis for 25 min, the chip was removed out of the chamber and rinsed with distilled water. For image and analysis, the chip was stained with 2.5  $\mu\text{g}/\text{mL}$  propidium iodide solution for 20 min. After being stained, the chip was rinsed with distilled water to remove excess stain (Figure 1C).

**Standard Comet Assay.** Single-cell suspension was prepared using enzyme disaggregation. Cells were placed in ice-cold medium to minimize cell aggregation and inhibit DNA repair. Cell density was adjusted to about  $2 \times 10^4$  cells/mL in phosphate-buffered saline. Cell suspension of 0.4 mL was mixed with 1.2 mL of 1% ultralow gelling temperature agarose at 20 °C. An amount of 100  $\mu\text{L}$  of cell suspension was pipetted onto the agarose-covered surface of a precoated slide. After the agarose gel was fully set, the following lysis and electrophoresis procedure was the same as the microfluidic comet assay as described.

**Genome Repair Capability Assay.** Cells were divided into four groups and loaded into four chips. Three of the four chips were submerged into 100  $\mu\text{M}$  hydrogen peroxide solution. The left one was used as the control group. After cells were treated with DNA damage agents, chips were carefully removed from the container and rinsed with buffer solution to remove excess hydrogen peroxide. Chips were placed in a bright room at 36 °C for different periods of time: 0, 30, and 60 min. Cell lysis and electrophoresis were performed as described previously.

**Optical Imaging.** An inverted fluorescence microscope (IX71, Olympus, Japan) with a CCD camera (Evolve 512, Photometrics, U.S.A.) was used for comet imaging. Cell loading was monitored under a 10 $\times$  objective lens (N.A. 0.3) with a filter cube of U-MWIB2 (460–490 nm band-pass filter, 505 nm dichroic mirror, 510 nm high-pass filter, Olympus, Japan). A cube of U-MWG2 (510–550 nm band-pass filter, 570 nm dichroic mirror, 590 nm high-pass filter, Olympus, Japan) was used for imaging comets.

**Data Analysis.** Acquired images were analyzed using Image Pro Plus 6.0 (MediaCybernetics, Silver Spring, MA, U.S.A.). The background image was taken from the blank agarose chip. The background image was subtracted from the image of comets. After removal of the image background using Image Pro Plus 6.0, the data analysis was performed using the softwares Cometscore 1.5 (TriTek, Sumerduck, VA) and Origin 7.5 (Northampton, MA, U.S.A.).

The images of comets were analyzed morphologically. The comet tail consists of relaxed loops and fragments, which stand for the damaged DNA. The tail DNA percentage was calculated as

$$P = \frac{F_{\text{tail}}}{F_{\text{tail}} + F_{\text{head}}} \times 100\% \quad (1)$$



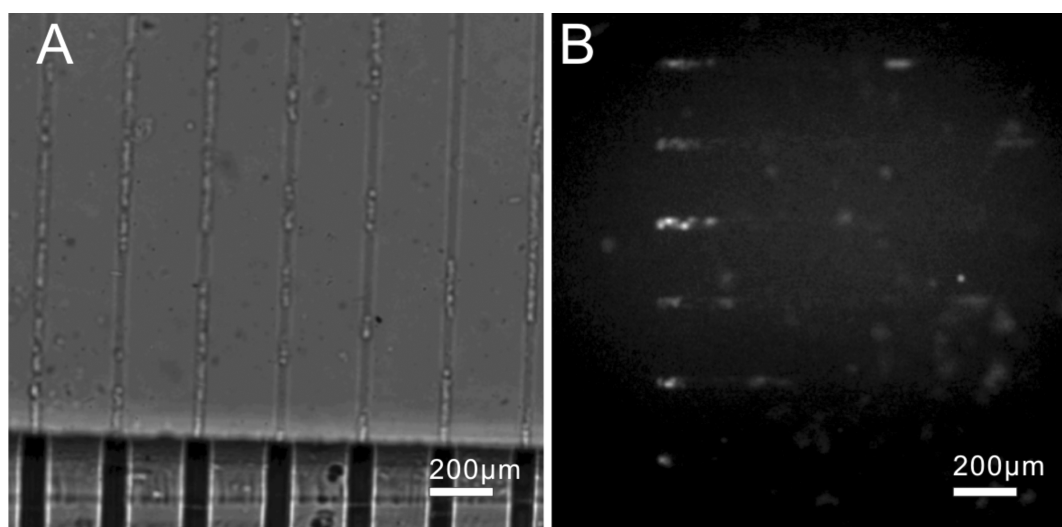


**Figure 2.** Cells loaded into the channels. (A) Optical image of cells after loading into the microchannels. (B) Fluorescence image of cells after loading into the microchannels.

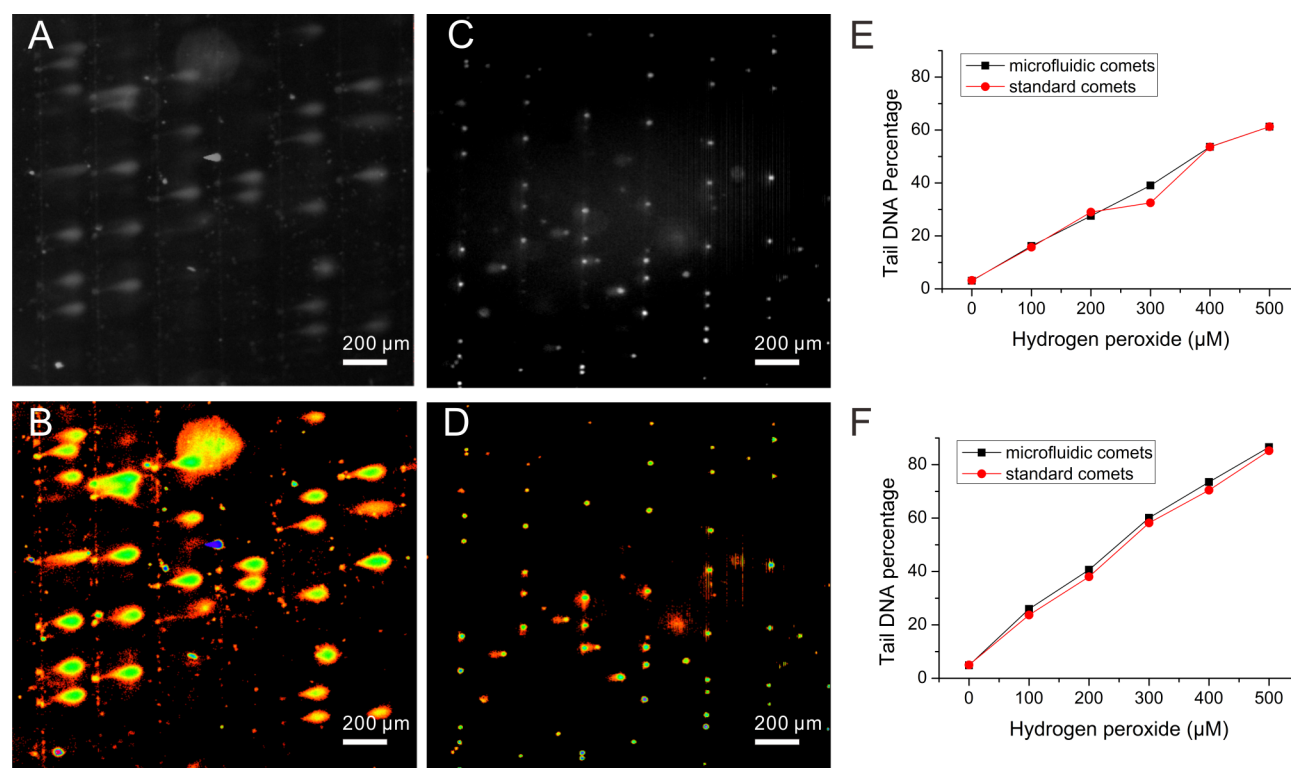


**Figure 3.** (A) Result of highly damaged cells after comet assay. (B) Pseudocolor image of panel A. (C) Result after comet assay in the control group. (D) Pseudocolor image of panel C. (E and F) Comparison of the traditional comet assay and the microfluidic comet assay of HeLa (E) and HepG2 (F) under various concentrations of hydrogen peroxide. Each data was the average of at least 50 individual comets.

where  $P$  represents the percentage of tail DNA and  $F_{\text{tail}}$  and  $F_{\text{head}}$  are the fluorescence intensities of tail DNA and head DNA, respectively.

## RESULTS AND DISCUSSION

**Automated Loading of Cell Arrays.** In the traditional comet assays, cells are dispersed in agarose randomly, which may lead to large numbers of unanalyzable cells due to the formation of cell mass. Cell patterning has been proposed for cell array formation to address the overlap issue. There are several existing cell patterning methods, including hydrostatic trapping,

dielectrophoresis, and suction from a side channel.<sup>59–61</sup> These methods involve the use of relatively large force produced by an external device for immobilizing cells, which might induce stress response of cells (change at the DNA transcription level), and further influence the cell resistance to DNA damage agents. For passive cell patterning such as microwell arrays and micropatterns, it is still a challenge to pattern cells with single-cell resolution.<sup>32,33</sup> Here, an agarose-based microfluidic chip is proposed for passive formation of a single-cell array and single-cell gel electrophoresis. A microchannel array was fabricated with agarose gel as the structure material through prototyping. A glass

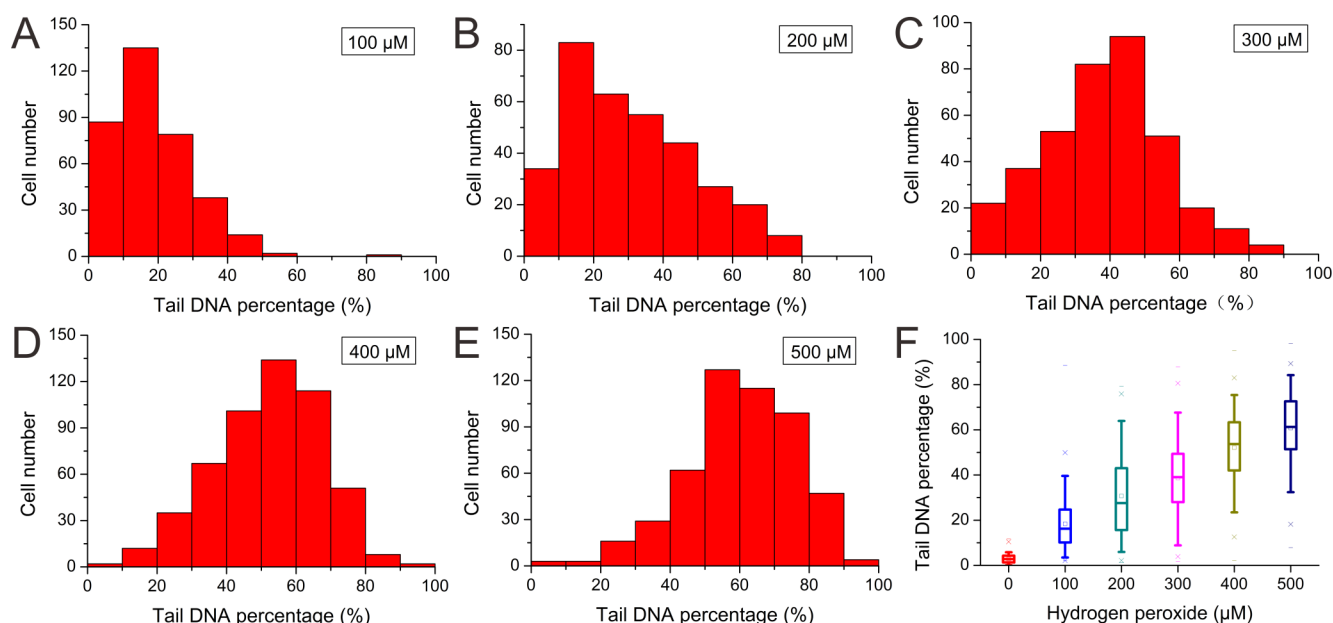


**Figure 4.** Statistical results of HeLa cells responding to different concentrated hydrogen peroxide solutions. Panels A–E represent the DNA damage distribution of at least 100 cells treated with a certain concentrated hydrogen peroxide solution for 7 min. (F) DNA damage of HeLa cells under the treatment of various concentrations of hydrogen peroxide. Box plots show the median of numbers of comets more than 100 as a middle line. The box edges show the lower and upper quartiles, the line out the box stands for the extent of the furthest data point within 150% of the interquartile range, and the fork means the largest and lowest amount.

slide was covered on top of the agarose layer to form the final device (Figure 1A). Cells were loaded into the channels by capillary effect and collected at the ends of the channels due to the permeability of agarose gel to water (Figure 1B). In consequence, cells were lined up in the parallel microchannels forming cell arrays. The loading process was finished in a few seconds, and a typical result is shown in Figure 2. After 5 min of incubation, collected cells were separated with each other due to the free diffusion of solution within the channels. The sample solution of  $10^5$  cells/mL prevented overlap on the chip in followed electrophoresis. Increasing cell density of the sample solution further improved the throughput of a chip. However, higher density of cell suspension also increased the probability of comets overlap. In comparison to random distribution of cells in the traditional methods, the ordered arrangement of cells in the microchannels largely prevented problems of cell overlap and maximized the use of space in the agarose-based microchip, which highly improved the throughput of a single chip.

**Agarose-Based Microfluidic Comet Assay.** Human cells are typically sensitive to free radicals known as reactive oxygen species (ROS) that randomly damage cellular constituents, such as oxidative DNA damage and destruction of DNA repair mechanism. The effect of ROS on cells could be measured by traditional comet assay, in which damaged DNA in an individual cell was quantitatively analyzed through agarose gel electrophoresis. In this paper, the developed agarose-based microfluidic chip was further used to analyze the effects of ROS on HeLa cells. After the array of HeLa cells was formed in the microchannels, 1% ultralow melting point agarose solution was pipetted on the chip to seal the microchannels. Cells in chips were then treated with hydrogen peroxide solution of various concentrations (0–500  $\mu\text{M}$ ) for 7 min. Following cell lysis, electrophoresis, and staining, the results of the agarose-based microfluidic comet assay were obtained. As shown in Figure 3, parts A and B, most of HeLa cells treated with hydrogen peroxide solution (400  $\mu\text{M}$ ) were

seriously damaged showing huge tails following comet heads (DNA trails) where cells located. Untreated HeLa cells were undamaged showing only comet heads without comet tails (Figure 3, parts C and D). These data showed various lengths of comet tails of HeLa cells after exposure to hydrogen peroxide. The lengths of the DNA tails might depend on the sensitivity of individual HeLa cell to hydrogen peroxide. Longer tails indicated more genomic DNA damage.

To validate the effectiveness of this proposed agarose-based microfluidic comet assay, we compared this developed microfluidic method with the traditional comet assay. Similarly, the responses of HeLa and HepG2 cells to hydrogen peroxide were also analyzed by traditional comet assay. Data in Figure 3, parts E (HeLa) and F (HepG2), showed average tail DNA percentage of at least 50 cells following exposure to varied concentrations of hydrogen peroxide by using these two methods. The correlation coefficients of linear regression ( $R^2$ ) for these two methods were both higher than 0.99. There was a little difference between the mean values of the two methods, indicating that the analytical results of the microfluidic comet assay were consistent with the standard method.

In addition, the throughput of this agarose-based microfluidic comet assay was calculated and evaluated. There were 100 channels on a simple 25 mm  $\times$  25 mm agarose chip. The length of each channel was 20 mm. The average distance between cells was about 200  $\mu\text{m}$ , and the distance between channels was also 200  $\mu\text{m}$ . Thus, 10 000 comets assays could be performed simultaneously (with a cell array density 25 comets/ $\text{mm}^2$ ). In comparison to the traditional comet assay [up to 400–1000 can be scored from a glass slide (25 mm  $\times$  75 mm) with a available comets density of 0.21–0.53 comets/ $\text{mm}^2$ ], our microfluidic approach has significantly improved the throughput (approximately 100-fold). Further, the cell array formation method reduced the number of unanalyzable cells due to the inhibition of cell overlap, which meant that it was much more sample-saving

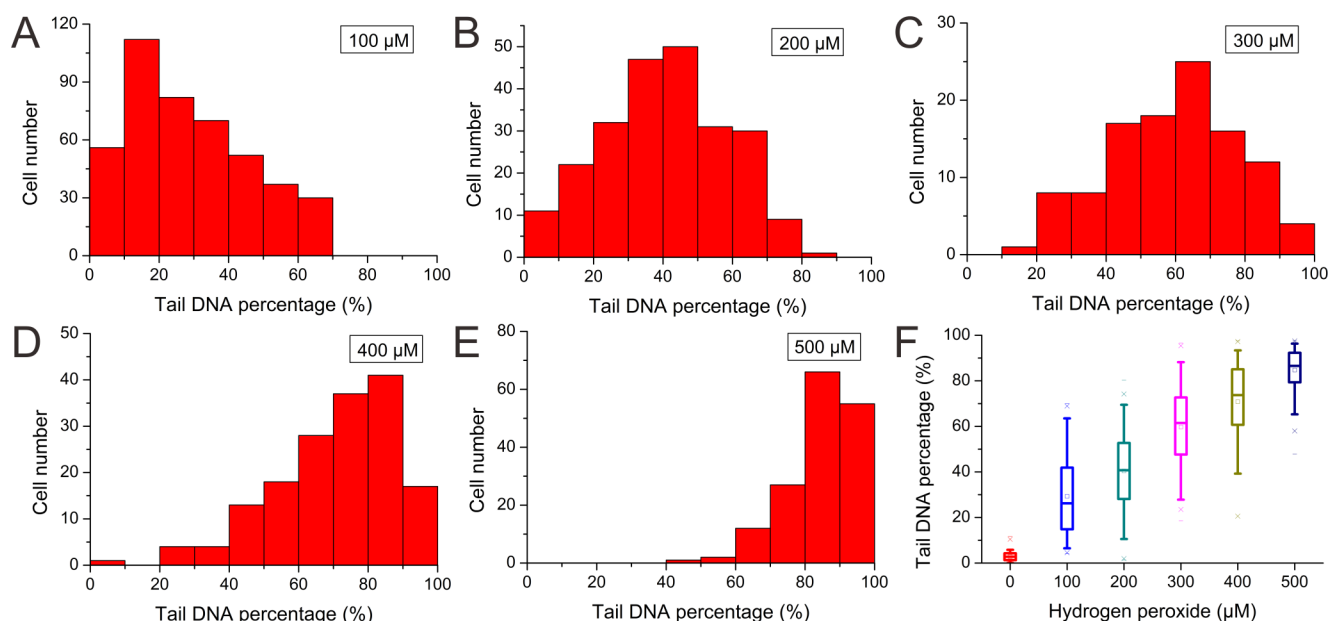


**Figure 5.** Statistical results of HepG2 cells responding to different concentrated hydrogen peroxide solutions. Panels A–E represent the DNA damage distribution of at least 100 cells treated with a certain concentrated hydrogen peroxide solution for 7 min. (F) DNA damage of HepG2 cells under the treatment of various concentrations of hydrogen peroxide. Box plots show the median of numbers of comets more than 100 as a middle line. The box edges show the lower and upper quartiles, the line out the box stands for the extent of the furthest data point within 150% of the interquartile range, and the fork means the largest and lowest amount.

than the standard comet assay. For reproducibility, a 7.9% coefficient of variation among chips was observed in the population average, which is less than the observed 11.65% coefficient of variation between slides in the traditional assay.<sup>62</sup> One of the reasons of poor repeatability in the standard comet assay is the inadequate mixing of agarose with cell suspension, which results in the varied concentration of agarose gels around single cells. The heterogeneity of pore structure within the agarose would disturb the electric field during electrophoresis, leading to low repeatability of the standard comet assay.<sup>63,64</sup> In the agarose-based microfluidic comet assay, cells were arranged on a solid-state chip made by uniform agarose gel, which confirmed the stability of the vertical electric field. Therefore, agarose-based microfluidic comet assay was more stable and had a better reproducibility than the standard comet assay.

**Quantitatively Analyzing the DNA Damage of Individual HeLa Cells.** For accurate evaluation of genomic DNA damage-induced cell death upon the treatment of hydrogen peroxide, the response of individual HeLa cells in the comet assay was quantitatively examined. The distribution of the tail DNA percentages of HeLa cells treated with 0–500 mM hydrogen peroxide are shown as Figure 4A–E. The figures showed that genomic DNA damage in the control group (0 mM hydrogen peroxide) had a mean tail DNA percentage between 2.78 and 3.43. With the treatment of increased concentration of hydrogen peroxide, the fraction of HeLa cells with high tail DNA percentage increased, ranging from 14.23 to 18.40 (mean value  $16.21 \pm 1.62$ , five groups with totally 1241 cells) under the treatment of 100 mM hydrogen peroxide, from 24.33 to 30.57 (mean value  $27.56 \pm 2.37$ , five groups with totally 1072 cells) under the treatment of 200 mM hydrogen peroxide, and from 53.96 to 67.26 (mean value  $61.28 \pm 5.03$ , five groups with totally 1307 cells) under the treatment of 500 mM hydrogen peroxide. Although for mean tail DNA percentage, the dose dependences were found to be linear in a range from 100 to 500 mM (Figure 4F), the results also indicated high heterogeneity among the cancer cell population.

Some cells exhibited extensive DNA damage while some others were not damaged even in high concentration of hydrogen peroxide (400 and 500 mM). Thus, the agarose-based microfluidic comet assay not only provided information about cell-to-cell differences of DNA damage within a cell population but also measured the average response of a cell population.

**Quantitatively Analyzing the DNA Damage of HepG2 Cells.** HeLa cells are relatively unspecialized epithelial cells. HepG2 cells are differentiated liver cell lines, containing drug-metabolizing enzyme activities similar to that in human hepatocytes.<sup>65</sup> To determine the difference between these two cell lines in response to ROS, we used the agarose-based microfluidic comet assay to quantify the amount of DNA damage of HepG2 cells under the treatment of hydrogen peroxide. By morphological analysis of the comets formed by damage DNA, obvious cells heterogeneity was observed in tail DNA percentage for HepG2 while exposing to various concentrations of hydrogen peroxide (100–500 mM) (Figure 5). In addition, linear dose dependency was also apparent in according to the mean tail DNA percentage. These results further confirmed that the tumor cells derived from one cell line had diverse replies to microenvironment changes. In comparison to HeLa cells (Figure 4F), HepG2 cells showed little difference in mean tail DNA percentage in response to the same concentration of hydrogen peroxide (Figure 5F), indicating hydrogen peroxide-induced DNA damage in these two cell lines was similar. However, cell heterogeneity in DNA damage of HepG2 cells under the treatment of 500 mM hydrogen peroxide appeared to be significantly less than that in HeLa cells (Figures 5E and 4E). Thus, the cell heterogeneity measured by this agarose-based microfluidic comet assay revealed the difference of the sensitivity to hydrogen peroxide between HepG2 and HeLa cells.

Cell heterogeneity is a widely observed phenomenon within a tumor mass of even a population of one cell line. Some cells in a tumor tissue exhibit strong resistance in response to the treatment of drugs. For example, a small population of “cancer

stem cells" was intrinsically more refractory to the effects of various anticancer drugs.<sup>66</sup> Accumulating evidence suggested that the resistance of a tumor to anticancer drug was often associated not with the average response among whole cell populations but with the response of a subpopulation of cells.<sup>67,68</sup> Therefore, the heterogeneity among the individual tumor cells acquired by this method might provide useful information about the resistance of the tumor to anticancer drugs.

**DNA Repair Capability Analysis.** Cells can avoid the accumulation of genome damage during growth by intact DNA repair systems. If the capacity of the cell's DNA repair could not suffice the rate of DNA damage, the accumulated genome errors would result in early senescence, apoptosis, or cancer. Inherited malfunction in DNA repair mechanism mostly results in premature aging, increased sensitivity to carcinogens, and correspondingly increased cancer risk. Likewise, the DNA repair regulates the resistance and sensitivity of cancer cells to anticancer drugs by the control of the DNA damage. Thus, the identification of DNA repair capacity of tumor cells was particularly important to predict the response of tumors to therapy. In this work, agarose-based microfluidic comet assay was further carried out for evaluating DNA repair capability by measuring the mean tail DNA percentage in HeLa and HepG2 cells.

HeLa cells were loaded onto four chips as described above. Three chips were set as the experiment groups while the other was the negative control. After the treatment of 100  $\mu$ M hydrogen peroxide, experiment groups were exposed to the light for 0 (acting as positive control in the experiment group), 30, and 60 min, respectively, at 37 °C to initiate the DNA repair mechanisms. As shown in Figure 6, the mean amount of tail DNA

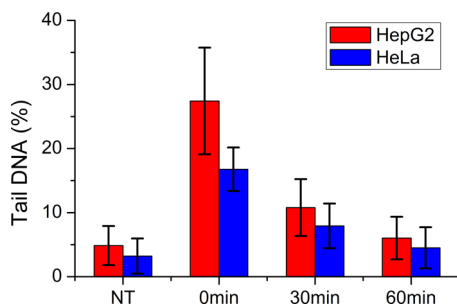


**Figure 6.** DNA repair kinetics of HeLa and HepG2 after being treated with 100  $\mu$ M hydrogen peroxide. The control group cells were treated with buffer (0  $\mu$ M hydrogen peroxide). DNA repair was performed at 37 °C with light on for 0, 30, and 60 min. Each data was the average of at least 50 individual comets.

of the cells in the negative control group was extremely low. With the treatment of ROS, serious DNA damage was observed for the cells in the positive control of experiment groups because no DNA repair occurred. A large part of DNA damage was successfully repaired for 30 min after the DNA damage. And almost all the DNA damage was repaired for 60 min. Likely, HepG2 cells showed very similar tendency in DNA repair capacity. These results indicated that our agarose-based microfluidic chip provided an effective method for accurate evaluation of the DNA repair.

## CONCLUSIONS

The comet assay has been widely used in a variety of biological and clinical applications by efficient measurement of genomic

DNA damage and repair at the single-cell level. In this work, we demonstrated a novel agarose-based microfluidic comets assay method, which extremely expanded the analytical throughput about 100-fold over the traditional comet assay strategy with more reproducibility. A microfluidic chip fabricated with agarose greatly facilitated the formation of a dense array of single cells and the subsequent DNA fragments separations of a single cell in parallel. Applications to analyzing the genomic DNA damage upon hydrogen peroxide and repair of two kinds of cancer cells such as HeLa and HepG2 cells were successfully achieved. It indicated that the developed agarose-based microfluidic comet array method was rapid, simple, highly reproducible, and of ultrahigh throughput, providing a highly efficient approach of choice for single-cell genomics.

## AUTHOR INFORMATION

### Corresponding Author

\*E-mail: bfliu@mail.hust.edu.cn. Phone: +86-27-87792203. Fax: +86-27-87792170.

### Notes

The authors declare no competing financial interest.

## ACKNOWLEDGMENTS

The authors gratefully acknowledge the financial support from the National Basic Research Program of China (2011CB910403) and the National Natural Science Foundation of China (21275060, 21075045).

## REFERENCES

- (1) Kitano, H. *Science* **2002**, *295*, 1662–1664.
- (2) Ideker, T.; Galitski, T.; Hood, L. *Annu. Rev. Genomics Hum. Genet.* **2001**, *2*, 343–372.
- (3) Feng, X.; Liu, X.; Luo, Q.; Liu, B. F. *Mass Spectrom. Rev.* **2008**, *27*, 635–660.
- (4) Liu, B. F.; Xu, B.; Zhang, G.; Du, W.; Luo, Q. *J. Chromatogr., A* **2006**, *1106*, 19–28.
- (5) Du, W.; Wang, Y.; Luo, Q.; Liu, B. F. *Anal. Bioanal. Chem.* **2006**, *386*, 444–457.
- (6) Dai, S.; Chen, S. *Mol. Cell. Proteomics* **2012**, *11*, 1622–1630.
- (7) Diks, S. H.; Peppelenbosch, M. P. *Trends Mol. Med.* **2004**, *10*, 574–577.
- (8) Irish, J. M.; Kotecha, N.; Nolan, G. P. *Nat. Rev. Cancer* **2006**, *6*, 146–155.
- (9) Ishoey, T.; Woyke, T.; Stepanauskas, R.; Novotny, M.; Lasken, R. S. *Curr. Opin. Microbiol.* **2008**, *11*, 198–204.
- (10) Lasken, R. S. *Curr. Opin. Microbiol.* **2007**, *10*, 510–516.
- (11) Navin, N.; Kendall, J.; Troge, J.; Andrews, P.; Rodgers, L.; McIndoo, J.; Cook, K.; Stepanky, A.; Levy, D.; Esposito, D.; Muthuswamy, L.; Krasnitz, A.; McCombie, W. R.; Hicks, J.; Wigler, M. *Nature* **2011**, *472*, 90–94.
- (12) Parkhomchuk, D.; Amstislavskiy, V.; Soldatov, A.; Ogryzko, V. *Proc. Natl. Acad. Sci. U.S.A.* **2009**, *106*, 20830–20835.
- (13) Yilmaz, S.; Singh, A. K. *Curr. Opin. Biotechnol.* **2012**, *23*, 437–443.
- (14) Zhang, K.; Martiny, A. C.; Reppas, N. B.; Barry, K. W.; Malek, J.; Chisholm, S. W.; Church, G. M. *Nat. Biotechnol.* **2006**, *24*, 680–686.
- (15) Ochman, H. *Environ. Microbiol.* **2007**, *9*, 7.
- (16) Walker, A.; Parkhill, J. *Nat. Rev. Microbiol.* **2008**, *6*, 176–177.
- (17) Bao, S.; Wu, Q.; McLendon, R. E.; Hao, Y.; Shi, Q.; Hjelmeland, A. B.; Dewhirst, M. W.; Bigner, D. D.; Rich, J. N. *Nature* **2006**, *444*, 756–760.
- (18) Gorgoulis, V. G.; Vassiliou, L. V.; Karakaidos, P.; Zacharatos, P.; Kotsinas, A.; Liloglou, T.; Venere, M.; Dittullo, R. A., Jr.; Kastrinakis, N. G.; Levy, B.; Kletsas, D.; Yoneta, A.; Herlyn, M.; Kittas, C.; Halazonetis, T. D. *Nature* **2005**, *434*, 907–913.
- (19) Jackson, S. P.; Bartek, J. *Nature* **2009**, *461*, 1071–1078.



- (20) Lu, T.; Pan, Y.; Kao, S. Y.; Li, C.; Kohane, I.; Chan, J.; Yankner, B. A. *Nature* **2004**, *429*, 883–891.
- (21) Zhou, B. B.; Elledge, S. J. *Nature* **2000**, *408*, 433–439.
- (22) Shuga, J.; Zeng, Y.; Novak, R.; Mathies, R. A.; Hainaut, P.; Smith, M. T. *Environ. Mol. Mutagen.* **2010**, *51*, 851–870.
- (23) Collins, A. R.; Oscoz, A. A.; Brunborg, G.; Gaivao, I.; Giovannelli, L.; Kruszewski, M.; Smith, C. C.; Stetina, R. *Mutagenesis* **2008**, *23*, 143–151.
- (24) Olive, P. L.; Banath, J. P. *Nat. Protoc.* **2006**, *1*, 23–29.
- (25) Tice, R. R.; Agurell, E.; Anderson, D.; Burlinson, B.; Hartmann, A.; Kobayashi, H.; Miyamae, Y.; Rojas, E.; Ryu, J. C.; Sasaki, Y. F. *Environ. Mol. Mutagen.* **2000**, *35*, 206–221.
- (26) Duez, P.; Dehon, G.; Kumps, A.; Dubois, J. *Mutagenesis* **2003**, *18*, 159–166.
- (27) Dusinska, M.; Collins, A. R. *Mutagenesis* **2008**, *23*, 191–205.
- (28) Godard, T.; Deslandes, E.; Sichel, F.; Poul, J. M.; Gauduchon, P. *Mutat. Res.* **2002**, *520*, 47–56.
- (29) Ostling, O.; Johanson, K. J. *Int. J. Radiat. Biol. Relat. Stud. Phys., Chem. Med.* **1987**, *52*, 683–691.
- (30) Santos, S. J.; Singh, N. P.; Natarajan, A. T. *Exp. Cell Res.* **1997**, *232*, 407–411.
- (31) Zhao, Q.; Le, X. C. *Anal. Bioanal. Chem.* **2007**, *387*, 45–49.
- (32) Wood, D. K.; Weingeist, D. M.; Bhatia, S. N.; Engelward, B. P. *Proc. Natl. Acad. Sci. U.S.A.* **2010**, *107*, 10008–10013.
- (33) Mercey, E.; Obeid, P.; Glaize, D.; Calvo-Munoz, M. L.; Guguen-Guillouzo, C.; Fouque, B. *Biomaterials* **2010**, *31*, 3156–3165.
- (34) Qiao, Y.; Wang, C.; Su, M.; Ma, L. *Anal. Chem.* **2012**, *84*, 1112–1116.
- (35) Feng, X.; Du, W.; Luo, Q.; Liu, B. F. *Anal. Chim. Acta* **2009**, *650*, 83–97.
- (36) Bennett, M. R.; Hasty, J. *Nat. Rev. Genet.* **2009**, *10*, 628–638.
- (37) Chronis, N.; Zimmer, M.; Bargmann, C. I. *Nat. Methods* **2007**, *4*, 727–731.
- (38) Chung, K.; Crane, M. M.; Lu, H. *Nat. Methods* **2008**, *5*, 637–643.
- (39) El-Ali, J.; Sorger, P. K.; Jensen, K. F. *Nature* **2006**, *442*, 403–411.
- (40) Fordyce, P. M.; Gerber, D.; Tran, D.; Zheng, J.; Li, H.; DeRisi, J. L.; Quake, S. R. *Nat. Biotechnol.* **2010**, *28*, 970–975.
- (41) Gerber, D.; Maerkl, S. J.; Quake, S. R. *Nat. Methods* **2009**, *6*, 71–74.
- (42) Lecault, V.; Vaninsberghe, M.; Sekulovic, S.; Knapp, D. J.; Wohrer, S.; Bowden, W.; Viel, F.; McLaughlin, T.; Jarandehi, A.; Miller, M.; Falconnet, D.; White, A. K.; Kent, D. G.; Copley, M. R.; Taghipour, F.; Eaves, C. J.; Humphries, R. K.; Piret, J. M.; Hansen, C. L. *Nat. Methods* **2011**, *8*, 581–586.
- (43) Lindstrom, S.; Andersson-Svahn, H. *Lab Chip* **2010**, *10*, 3363–3372.
- (44) Yager, P.; Edwards, T.; Fu, E.; Helton, K.; Nelson, K.; Tam, M. R.; Weigl, B. H. *Nature* **2006**, *442*, 412–418.
- (45) Dalerba, P.; Kalisky, T.; Sahoo, D.; Rajendran, P. S.; Rothenberg, M. E.; Leyrat, A. A.; Sim, S.; Okamoto, J.; Johnston, D. M.; Qian, D.; Zabala, M.; Bueno, J.; Neff, N. F.; Wang, J.; Shelton, A. A.; Visser, B.; Hisamori, S.; Shimonon, Y.; van de Wetering, M.; Clevers, H.; Clarke, M. F.; Quake, S. R. *Nat. Biotechnol.* **2011**, *29*, 1120–1127.
- (46) Spiller, D. G.; Wood, C. D.; Rand, D. A.; White, M. R. *Nature* **2010**, *465*, 736–745.
- (47) Salehi-Reyhani, A.; Kaplinsky, J.; Burgin, E.; Novakova, M.; deMello, A. J.; Templer, R. H.; Parker, P.; Neil, M. A.; Ces, O.; French, P.; Willison, K. R.; Klug, D. *Lab Chip* **2011**, *11*, 1256–1261.
- (48) Kumaresan, P.; Yang, C. J.; Cronier, S. A.; Blazej, R. G.; Mathies, R. A. *Anal. Chem.* **2008**, *80*, 3522–3529.
- (49) Novak, R.; Zeng, Y.; Shuga, J.; Venugopalan, G.; Fletcher, D. A.; Smith, M. T.; Mathies, R. A. *Angew. Chem., Int. Ed.* **2011**, *50*, 390–395.
- (50) Toriello, N. M.; Douglas, E. S.; Thaitrong, N.; Hsiao, S. C.; Francis, M. B.; Bertozzi, C. R.; Mathies, R. A. *Proc. Natl. Acad. Sci. U.S.A.* **2008**, *105*, 20173–20178.
- (51) Blazej, R. G.; Kumaresan, P.; Cronier, S. A.; Mathies, R. A. *Anal. Chem.* **2007**, *79*, 4499–4506.
- (52) Blazej, R. G.; Kumaresan, P.; Mathies, R. A. *Proc. Natl. Acad. Sci. U.S.A.* **2006**, *103*, 7240–7245.
- (53) Liu, C. N.; Toriello, N. M.; Mathies, R. A. *Anal. Chem.* **2006**, *78*, 5474–5479.
- (54) Liu, P.; Li, X.; Greenspoon, S. A.; Scherer, J. R.; Mathies, R. A. *Lab Chip* **2011**, *11*, 1041–1048.
- (55) Liu, P.; Mathies, R. A. *Trends Biotechnol.* **2009**, *27*, 572–581.
- (56) Liu, P.; Seo, T. S.; Beyor, N.; Shin, K. J.; Scherer, J. R.; Mathies, R. A. *Anal. Chem.* **2007**, *79*, 1881–1889.
- (57) Toriello, N. M.; Liu, C. N.; Blazej, R. G.; Thaitrong, N.; Mathies, R. A. *Anal. Chem.* **2007**, *79*, 8549–8556.
- (58) Yeung, S. H.; Liu, P.; Del Bueno, N.; Greenspoon, S. A.; Mathies, R. A. *Anal. Chem.* **2009**, *81*, 210–217.
- (59) Di Carlo, D.; Lee, L. P. *Anal. Chem.* **2006**, *78*, 7918–7925.
- (60) Gray, D. S.; Tan, J. L.; Voldman, J.; Chen, C. S. *Biosens. Bioelectron.* **2004**, *19*, 1765–1774.
- (61) Werdich, A. A.; Lima, E. A.; Ivanov, B.; Ges, I.; Anderson, M. E.; Wiksw, J. P.; Baudenbacher, F. J. *Lab Chip* **2004**, *4*, 357–362.
- (62) Zainol, M.; Stoute, J.; Almeida, G. M.; Rapp, A.; Bowman, K. J.; Jones, G. D. *Nucleic Acids Res.* **2009**, *37*, e150.
- (63) Olive, P. L. *Methods Mol. Biol.* **2002**, *203*, 179–194.
- (64) Olive, P. L.; Johnston, P. J.; Banath, J. P.; Durand, R. E. *Nat. Med.* **1998**, *4*, 103–105.
- (65) Doostdar, H.; Demoz, A.; Burke, M. D.; Melvin, W. T.; Grant, M. H. *Xenobiotica* **1990**, *20*, 435–441.
- (66) Trumpp, A.; Wiestler, O. D. *Nat. Clin. Pract. Oncol.* **2008**, *5*, 337–347.
- (67) Chang, H. H.; Hemberg, M.; Barahona, M.; Ingber, D. E.; Huang, S. *Nature* **2008**, *453*, 544–547.
- (68) Sharma, S. V.; Lee, D. Y.; Li, B.; Quinlan, M. P.; Takahashi, F.; Maheswaran, S.; McDermott, U.; Azizian, N.; Zou, L.; Fischbach, M. A.; Wong, K. K.; Brandstetter, K.; Wittner, B.; Ramaswamy, S.; Classon, M.; Settleman, J. *Cell* **2010**, *141*, 69–80.